Synthesis of PEDOT:PSS Brushes Grafted from Gold Using ATRP for Increased Electrochemical and Mechanical Stability

Jason X. Tuermer-Lee[1], Allison Lim[1], Louis Ah[1], Rachel Blau[1], Yi Qie[1], Wade Shipley[2], Laure V. Kayser[3,4], Samantha M. Russman[5], Andrea R. Tao[1,2], Shadi A. Dayeh[5], and Darren J. Lipomi[*1,2]

[1] Department of NanoEngineering, University of California, San Diego
9500 Gilman Dr, Mail Code 0448, La Jolla, CA 92093-0448, USA

[2] Materials Science and Engineering, University of California, San Diego
9500 Gilman Dr, Mail Code 0418, La Jolla, CA 92093-0418, USA

[3] Department of Materials Science and Engineering, University of Delaware
201 Dupont Hall, Newark, DE 19716-3106, USA

[4] Department of Chemistry and Biochemistry, University of Delaware
102 Brown Laboratory, Newark, Delaware, 19716-3106, USA

[5] Integrated Electronics and Biointerfaces Laboratory, Department of Electrical and Computer Engineering, University of California, San Diego
9736 Engineers Ln, La Jolla, CA 92093, USA

[*]Author to whom correspondence should be addressed: dlipomi@ucsd.edu

Supporting Information Placeholder

ABSTRACT: We report PEDOT:PSS brushes grafted from gold using surface-initiated atom-transfer radical polymerization (SI-ATRP) which demonstrate significantly enhanced mechanical stability against sonication and electrochemical cycling compared to spin-coated analogs, as well as lower impedances than bare gold at frequencies from 0.1–10^5 Hz. These results suggest SI-ATRP PEDOT:PSS to be a promising candidate for use in microelectrodes for neural activity recording. Spin-coated, electrodeposited, and drop-cast PEDOT:PSS have already been shown to reduce impedance and improve biocompatibility of microelectrodes, but the lack of strong chemical bonds of the physisorbed polymer film to the metal leads to disintegration under required operational stresses including cyclic mechanical loads, abrasion, and electrochemical cycling. Rather than modifying the metal electrode or introducing crosslinkers or other additives to improve the stability of the polymer film, this work chemically tethers the polymer to the surface, offering a simple, scalable solution for functional bioelectronic interfaces.

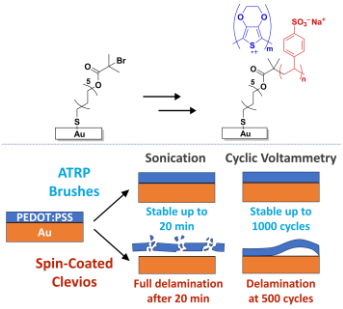

The growing interest in wearable and implantable electrodes for bioelectronic applications has propelled the development of smaller and smaller electrodes ("microelectrodes")[1–3]. Microelectrodes offer high spatial resolution and sensitivity and provide the ability to both record and stimulate highly localized areas. Traditionally, biocompatible metals like platinum, platinum-iridium, and stainless steel are used in clinical applications that require electrophysiological recording and stimulation[4,5]. However, small metal electrodes suffer from high electrochemical impedance with biological tissue which increases the electrochemical noise of electrodes and impairs their sensitivity[6,7]. Conductive polymers offer a solution that can be integrated with current microelectrode fabrication techniques, both lowering impedance and creating a surface more mechanically compatible with the surrounding tissue[3,8]. In particular, the mixed electronic/ionic conduction mechanism of the polyelectrolyte complex poly(3,4-ethylenedioxythiophene):poly(styrene sulfonate) (PEDOT:PSS) exhibits a high volumetric capacitance and, as a hydrated solid, low impedance with biological tissues. Electrodeposition or spin-coating of PEDOT:PSS onto gold microelectrodes lowers the impedance and increases charge injection capacity compared to bare metal electrodes[7,9–12]. Polymer coated metal electrodes seem to offer a biocompatible option for long-term neural electrodes. While studies have shown that the electrodes are stable under biologically relevant conditions, the polymers—which are physisorbed—are not bound chemically to the gold surface. Thus, over time and with repeated applied current these polymers can

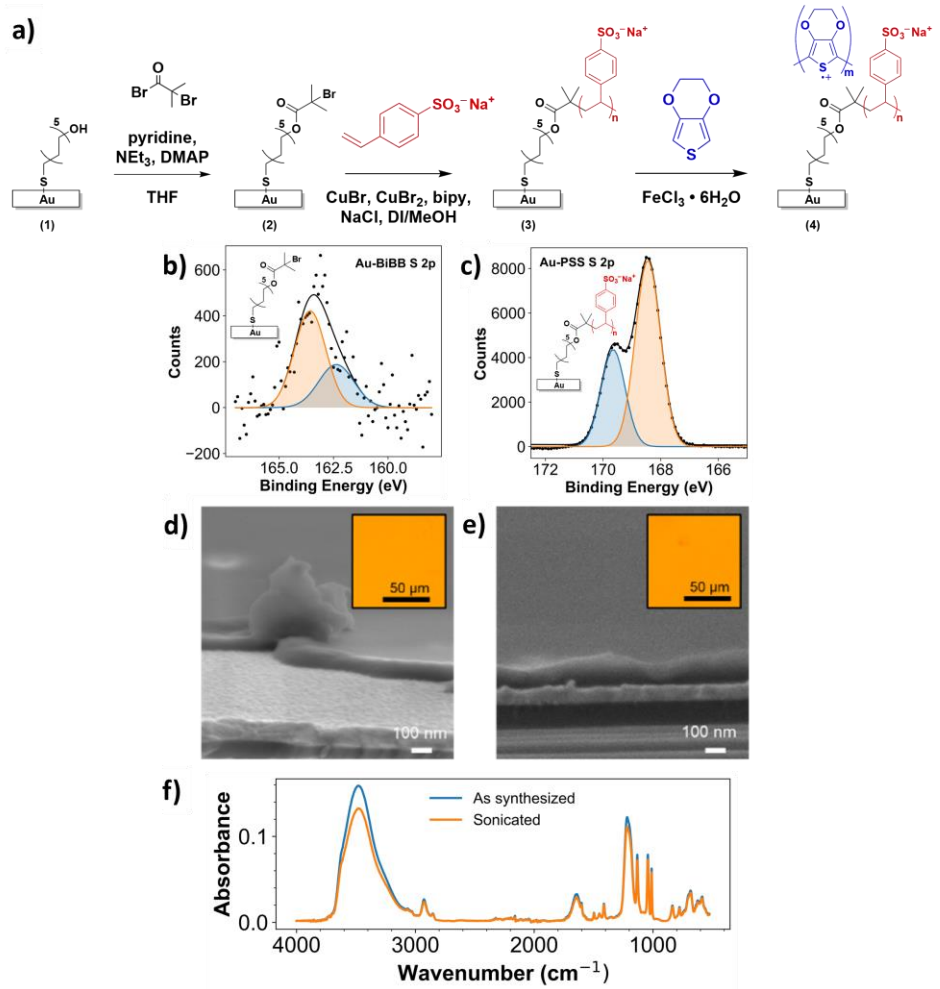

Figure 1. Chemically grafted PEDOT:PSS brushes on gold. (a) Reaction scheme for synthesis of grafted PEDOT:PSS brushes from an immobilized initiator (1) and (2). NaPSS brushes were grown from the gold-bound initiator (3) and used as a scaffold for the polymerization of EDOT into PEDOT (4). (b) The S 2p XPS spectra confirmed that the initiator was bound to the gold surface via peaks at 163.5 and 162.3 eV. (c) The S 2p spectra for PSS bound to gold also shows characteristic double from the sulfonate group. The PSS brushes bound to gold were stable after 20 min of sonication, as shown by SEM micrographs before (d) and after (e). Optical microscopy images of the PSS film on gold before (d) and after (e) sonication are included in the upper right corners of the SEM images. (f) The FTIR spectra of the sonicated sample also indicates the presence of PSS on the surface, though the slight decrease in intensity after sonication indicates a small amount of PSS was removed from the surface by sonication.

degrade and lose adhesion to the metal electrode. Patterning the metal electrode can improve adhesion and stability of PEDOT:PSS layers, but ideally the polymer should be chemically bound to the surface.

PEDOT has been explored as a coating for metal microelectrodes and as a free-standing electrode to reduce impedance and improve compatibility with surrounding tissue. Abidian et al. explored PEDOT nanotubes on gold microelectrodes (1250 μm^2) and found that the PEDOT nanotubes significantly reduced the impedance at 1 kHz, from 800 kΩ in bare gold to 4 kΩ (~5 kΩ · μm^2)[13]. However, the smooth gold surfaces and lack of chemically bound PEDOT rendered these nanorods susceptible to delamination. Ganji et al.[14] and Nick et al.[10] addressed the delamination and stability of PEDOT:PSS coatings in an examination of spin-coated, electrodeposited, and drop-casted PEDOT:PSS films on nanostructured gold microelectrodes. The addition of nanopillar structures on gold increased the adhesion, primarily by increasing the total interfacial area. Ganji et al. reported an impedance of 13.05 kΩ (7854 μm^2, ~1.02 x 10^5 kΩ · μm^2) for spin-coated samples and 9.72 kΩ (7854 μm^2, 7.6 x 10^4 kΩ · μm^2) for electrodeposited samples. The electrodeposited samples also displayed higher stability than the spin-coated samples[14]. In comparison, the drop-casted PEDOT:PSS electrodes fabricated by Nick et al. had an impedance of 36.82 kΩ (706 μm^2, ~2.6 x 10^4 kΩ · μm^2), but no long-term stability was reported[11]. This recent literature has shown that PEDOT:PSS can effectively lower the impedance of gold electrodes, but there is still significant room to increase the stability of the PEDOT:PSS overlayers. For this reason, PEDOT:PSS in frequently blended with the crosslinker (3-glycidoxypropyl)trimethoxysilane (GOPS) or other additives in bioelectronics applications in order to increase stability and prevent dissolution or delamination in aqueous environments[15–18]. Other recent work on improving PEDOT:PSS thin-film adhesion has explored the use of hydrophilic polymer adhesive layers[19], PEGylated crosslinkers that impart greater conductive properties than GOPS[20], and the use of iridium oxide and nanostructured

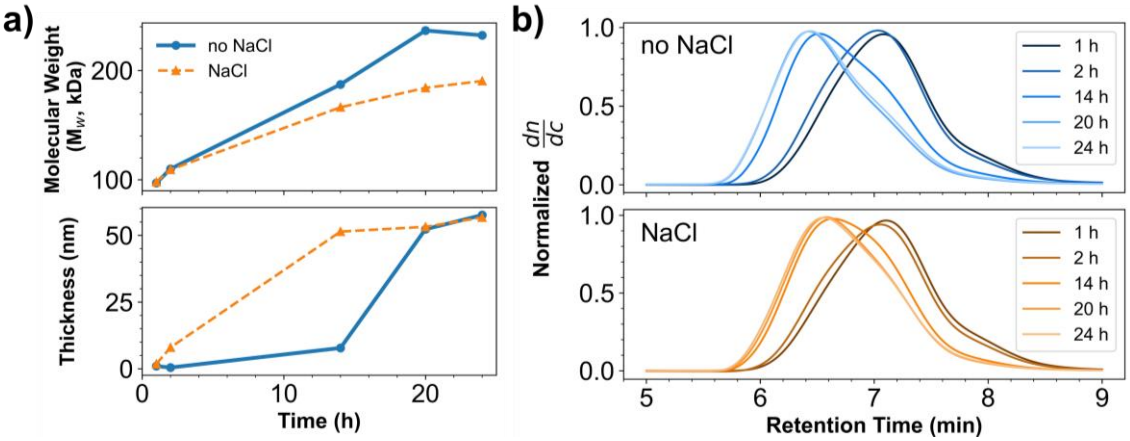

Figure 2. Characterization of free PSS and estimation of molecular weight. (a) The molecular weight of the free polymer increases then slows approaching 24 h, likely due to diffusion of oxygen into the system. The thickness of the brushes follows a similar trend. The addition of NaCl (dashed orange) seemed to increase the growth rate of brushes on the surface but did not have significant effect on the dispersity (b) of the free polymer.

platinum as adhesion promoters[21]. However, these methods introduce other concerns of additives leaching out of the material with time and affecting the electrode performance and biocompatibility.

Alternatively, surface-initiated polymerization from metallic films presents the opportunity to chemically bind a conductive polymer like PEDOT:PSS to a noble metal microelectrode surface. By selectively initiating a metal surface, such as gold, PEDOT:PSS can be grown or grafted from a surface or grafted to a surface. In both of these techniques—"grafting from" and "grafting to"—functional groups on the polymer or the surface are chemically bound, increasing the stability of the grafted polymer. This method avoids the use of additives and does not involve nanostructuring of the gold substrate. Electrochemically grafting (or "electrografting") PEDOT to solid conducting substrates such as platinum and gold has been explored as a method of covalently tethering the polymer film to the substrate[22,23], though prior work has not explored the use of this method for the covalent binding of PSS brushes. Previous work grafting PSS to or from metal surfaces has been explored, with a preference to grafting PSS from a surface to improve grafting density[24–29]. However, these techniques rely on a two-step process to synthesize PSS—polymerization of styrene followed by sulfonation[25,28,29]. This process may lead to incomplete sulfonation and exposes the surfaces to acid. Acidic conditions are too harsh for the intended application in devices containing microelectrode arrays, which often contain other organic polymers, which may be damaged. The one example of polymerization of sodium styrene sulfonate from a gold surface extensively characterized the surface morphology and explored reaction conditions but did not provide electrochemical analysis or use the brushes as a scaffold for PEDOT:PSS[27]. Grafting of PSS and other mixed conjugated/electrolyte brushes using SI-ATRP has also been explored on conductive substrates other than gold such as ITO (indium tin oxide) as a means of improving durability[30], but this work did not use PEDOT as the conductive polymer. In this work, we take advantage of surface-initiated atom transfer radical polymerization (SI ATRP) to grow polystyrene sulfonate (PSS) brushes from gold surfaces to demonstrate their stability and potential for application in microelectrode array coatings. Using aqueous conditions and incorporating solution deposition of PEDOT, we characterize the electrochemical properties of PEDOT:PSS brushes fabricated via SI-ATRP of sodium styrene sulfonate.

Binding ATRP initiators to gold surfaces can be done two ways: a one-step surface assembled monolayer of the ATRP initiator[31,32] or a two-step surface assembled monolayer of a hydroxy terminated thiol followed by an additional reaction, as summarized in **Figure 1a** [33,34]. The one step reaction may lead to a higher density of initiator groups since the two step reaction may not occur in 100% yield, leaving unreacted hydroxy groups at the surface[33]. However, the one-step process requires uneconomical work up conditions, so we opted for the more streamlined two-step process. A hydroxy terminated SAM was formed by soaking the gold surface in 11-mercaptoundecanol (MUD). The surface was rinsed then underwent a nucleophilic addition/elimination reaction with α-bromoisobutyryl bromide to form the ATRP initiator. This two-step process does not require any additional work up besides rinsing with ethanol and water and has been shown to form dense polymer brushes[34,35].

Polystyrene sulfonate (PSS) has been polymerized from surfaces as a polyelectrolyte brush and as a scaffold for PEDOT. However, generally PSS is synthesized by sulfonating polystyrene brushes[25,28,29], leading to incomplete sulfonation and subjecting the substrate to harsh, acidic conditions. Alternatively, PSS terminated with reaction end groups, like thiols, can be synthesized and grafted *to* a surface, but this process leads to a lower grafting density. In order to retain high grafting density and avoid harsh sulfonation conditions, sodium styrene sulfonate (NaSS) can be directly polymerized into PSS from a surface-bound initiator. Surface initiated atom transfer polymerization (SI-ATRP) would allow for polymerization of NaSS in aqueous conditions with control over the molecular weight and thickness of the brushes due to the living nature of ATRP. Polymerization of NaSS in solution via ATRP has been explored, indicating that surface initiated ATRP of NaSS is feasible[36]. Recent work in activators regenerated by electron transfer (ARGET) ATRP posits ATRP can be made much more oxygen tolerant through the introduction of an appropriate reducing agent. Oxygen tolerance improves the scalability of this type of polymerization[37–40]. ARGET ATRP of NaSS from titanium surfaces has been studied using ascorbic acid as the reducing agent, further supporting the possibility of SI-ATRP of NaSS on gold surfaces[26].

In this work, PSS brushes were grafted from gold surfaces by immobilizing an ATRP initiator on a gold surface then polymerizing NaSS, as shown in **Figure 1a.** Chemically bound initiator was shown by the S 2p XPS spectra in **Figure 1b** (raw data shown as a

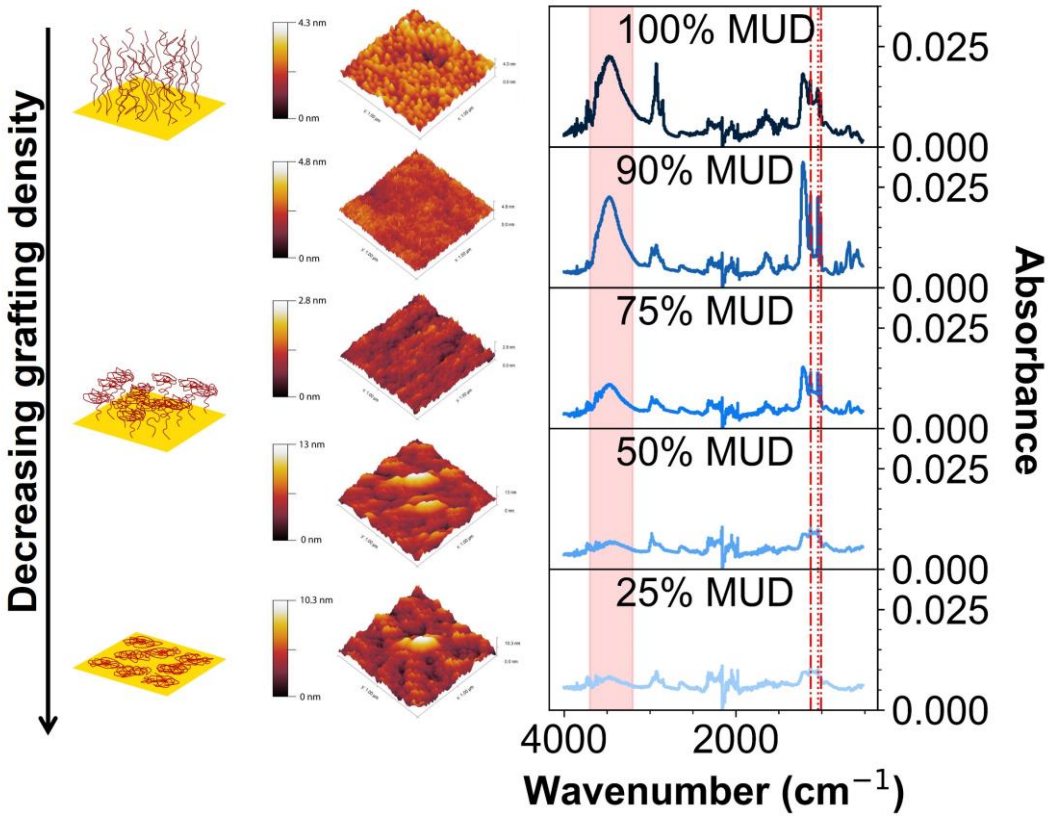

Figure 3. Changes in brush morphology were observed via AFM by manipulating the grafting density. The grafting density was reduced by replacing a fraction of the initiated surface with a non-reactive alkane. A decrease in of the FTIR signal at 1130, 1043, and 1011 cm^{-1} indicated a decrease in PSS grafted to the surface. The OH stretching peak between 3200-3700 cm^{-1} also decreased as the amount of hydroscopic PSS on the surface decreases. As the amount of PSS grafted from the surface decreased, a distinct change in morphology of the brushes was observed via AFM, from brush at 100% initiator to pancake like between 25-50% initiator.

scatter plot with the overall fitted curve shown in black) with the presence of a doublet at 163.5 and 162.3 eV[44]. Successful synthesis of PSS brushes from the immobilized ATRP initiator could be observed qualitatively with an increase in hydrophilicity of the surface and was confirmed by characteristic peaks at 1130 and 1011 cm^{-1} (benzene vibration), and 1043 cm^{-1} (symmetric sulfonate vibration) in FTIR spectra[45] and a doublet at 169.6 and 168.4 eV in the S 2p XPS spectra (**Figure 1c-d**)[24,46]. Sonicating the PSS-Au samples for 20 min in water showed no major changes via optical microscopy, SEM, or FTIR signal, as seen in **Figure 1d-f**. In comparison, spin-coated PEDOT:PSS (Clevios™ PH1000) washes off of gold immediately upon rinsing with water, whereas spin-coated and crosslinked PEDOT:PSS (Clevios™ PH1000 with 0.2 wt% GOPS) was stable for up to 20 minutes of sonication (**Supporting Information, Figure S2d-f**).

The molecular weight of PSS brushes was estimated using free polymer synthesized in the same reaction vessel. The growth of the free polymer chains did not appear to be living as the molecular weight plateaued as the reaction approached 24 h, as seen in **Figure 2a**. In an attempt to improve the "living-ness" and reproducibility of the polymerization, NaCl was added. Introducing a salt reduces Cu(I) disproportionation and reduces termination by preventing loses due to Cu complexing with the charged sulfonate group on NaSS[40]. Adding NaCl seemed to increase the growth rate of the PSS brushes, as evidenced by the thicker brushes between 2 and 20 h in **Figure 2a**. The molecular weight of free polymer was also lower when synthesized with NaCl, suggesting less termination due to recombination, however, the PDI was similar between polymers synthesized with and without NaCl, seen by the GPC traces in **Figure 2b**. NaCl did not seem to have a significant effect on the thickness of the PSS brushes or the molecular weight of the free polymers.

The morphology of the PSS brushes is highly dependent on the grafting density of the polymer; however, it is difficult to quantitatively measure the density of polymers grafted from a surface. While we could not characterize the density of initiator per surface, we could still observe changes in grafting density by introducing non-reactive alkanethiols. Instead of synthesizing hydroxy terminated surfaces from MUD, as seen in **Figure 1a (1)**, we created a surface terminated by a mixture of hydroxyl and alkyl groups. The alkyl groups would not react further with the initiator or PSS, effectively controlling the grafting density. As we increased the amount of non-reactive alkane and decreased the grafting density, the morphology of the brushes changed from densely packed, upright brushes, to flattened, pancake-like (**Figure 3**). Changes in FTIR spectra were also consistent with less PSS present on surfaces with less initiator. The OH stretching vibration between 3700-3200 cm^{-1} decreased with decreasing initiator concentration (% MUD). PSS is hygroscopic, so lower amounts of PSS on the surface would be correlated to less water and less intense OH stretching. Lower

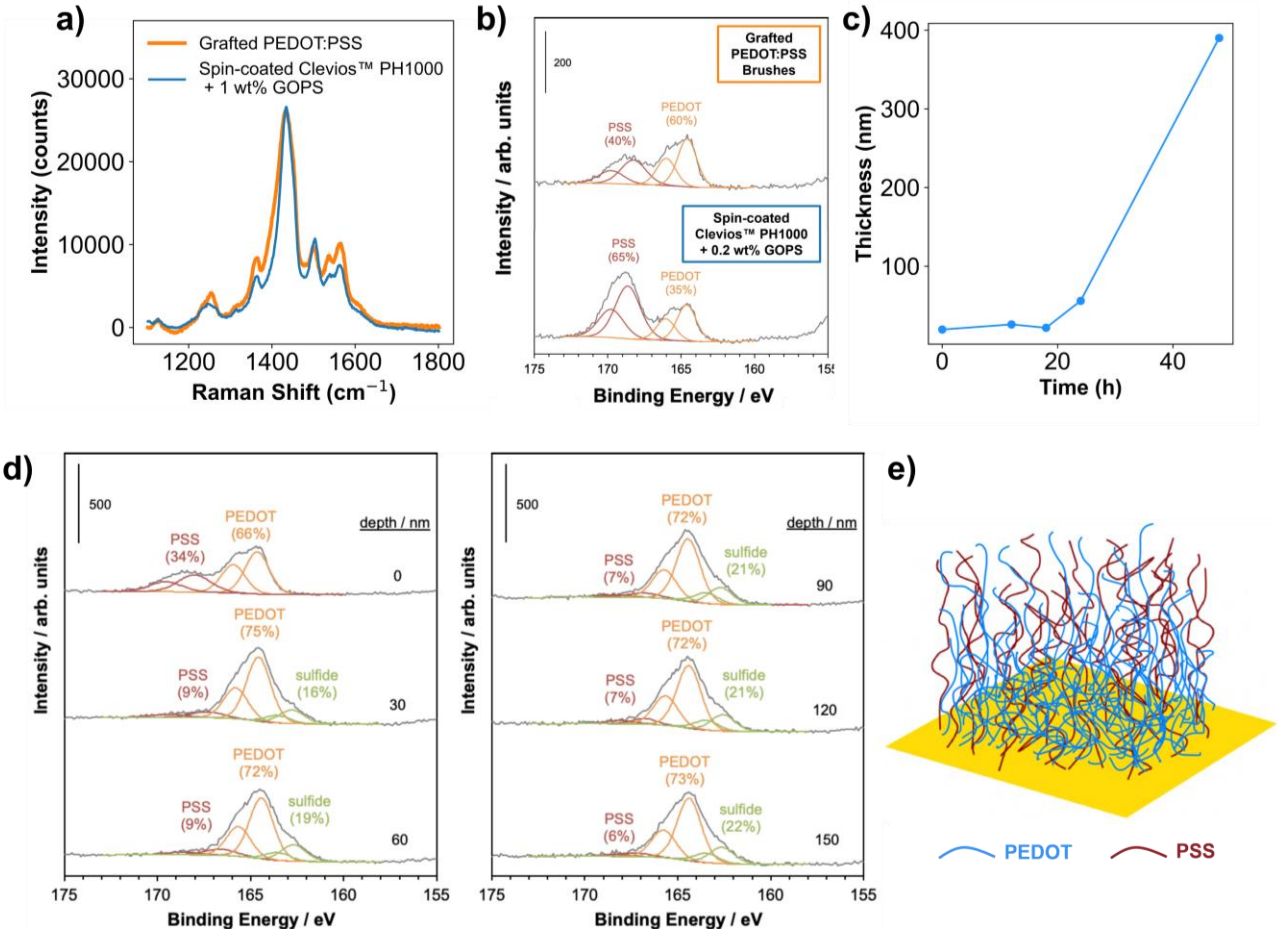

Figure 4. (a) Raman spectra of PEDOT:PSS grafted from gold (orange) with characteristic peaks at 1366, 1435, 1501, and 1562 cm^{-1}, plotted with Raman spectra of spin-coated Clevios™ PH1000 with 1 wt% GOPS crosslinker (blue) with characteristic peaks at 1361, 1434, 1501, and 1564 cm^{-1}. (b) The S 2p XPS spectra compare the amount of PEDOT to PSS for grafted PEDOT:PSS (top) and spin-coated Clevios™ PH1000 with 0.2 wt% GOPS (bottom). Integration approximated the PEDOT:PSS ratios in mol:mol as 60:40 and 35:65 for the grafted and spin-coated samples, respectively. (c) The thickness of the PEDOT:PSS films could be simply controlled through the reaction time of EDOT copolymerization. Increasing the reaction time significantly increased the thickness of samples, from 5 nm of added thickness after 12 h to 50 nm after 24 h. (d) The S 2p XPS depth-profiling spectra compare the relative amounts of PEDOT and PSS (in mol%) of the grafted brushes at sputter depths ranging from 0–150 nm. These results show that PEDOT deeply penetrates the PSS brushes and is not limited to the film surface. A graphical illustration of the film highlighting the interpenetration of PEDOT is shown in (e).

FTIR signals at key frequencies for the benzene and sulfonate group indicate less PSS is present, demonstrating that manipulation of the grafting density was successful. We were thus able to confirm that the brushes synthesized with 100% initiator were densely packed and brush-like.

The PSS brushes were used as a scaffold to polymerize EDOT into conductive PEDOT. PEDOT could be observed optically through the presence of a blue film on the surface and signature Raman shifts (**Figure 4a**). at 1366 cm^{-1} (C_α-$C_{\alpha'}$), 1435 cm^{-1} (C_β-C_β), 1501 cm^{-1} , (C_α=C_β), and 1562 cm^{-1} (C_α=C_β) In comparison, spin-coated Clevios™ PH1000 with 1 wt% GOPS crosslinker had similar characteristic peaks at 1361 cm^{-1} (C_α-$C_{\alpha'}$), 1434 cm^{-1} (C_β-C_β), 1501 cm^{-1} , (C_α=C_β), and 1564 cm^{-1} (C_α=C_β). The ratio of PEDOT:PSS was estimated by integrating the S 2p XPS spectra (**Figure 4b**). The doublet at lower binding energy (163.6 and 164.8 eV) was assigned to the sulfur atoms in PEDOT and the doublet at higher binding energy (167.6 and 168.8 eV) was associated with the sulfonate group on PSS[47–49]. The grafted PEDOT:PSS had a ratio of 60:40 (mol:mol) compared to the measured 35:65 of spin-coated Clevios™ PH1000 with 0.2 wt% GOPS. The higher ratio of PEDOT in the grafted brushes is important to note, as higher PEDOT ratios are typically associated with increased conductivities due to the decreased energy barrier for interchain and interdomain charge hopping[50]. **Figure 4c** shows how the grafting process allows for control over the thickness of the PEDOT:PSS films simply through the reaction time of the EDOT polymerization. To better determine the morphology of the PEDOT:PSS brushes, XPS depth-profiling was conducted at sputter depths ranging from 0–150 nm (**Figure 5d**). Integration of the S 2p peaks to determine the ratio of PEDOT to PSS at varying film depths revealed that the PEDOT chains deeply penetrate the PSS brushes and are not limited to the surface. In fact, the data reveal that PSS is most strongly present at the film surface. These results indicate that PEDOT diffuses deeply into the PSS brushes during aqueous solution deposition, causing the brushes to expand from a thickness of roughly 50 nm to 150 nm before and after aqueous PEDOT deposition, respectively. A graphical illustration of this morphology is shown in **Figure 5e**.

An image of a grafted PEDOT:PSS sample highlighting the uniformity of the surface is included in **Figure S1** of the Supporting Information. Sonicating the grafted PEDOT:PSS sample for 20

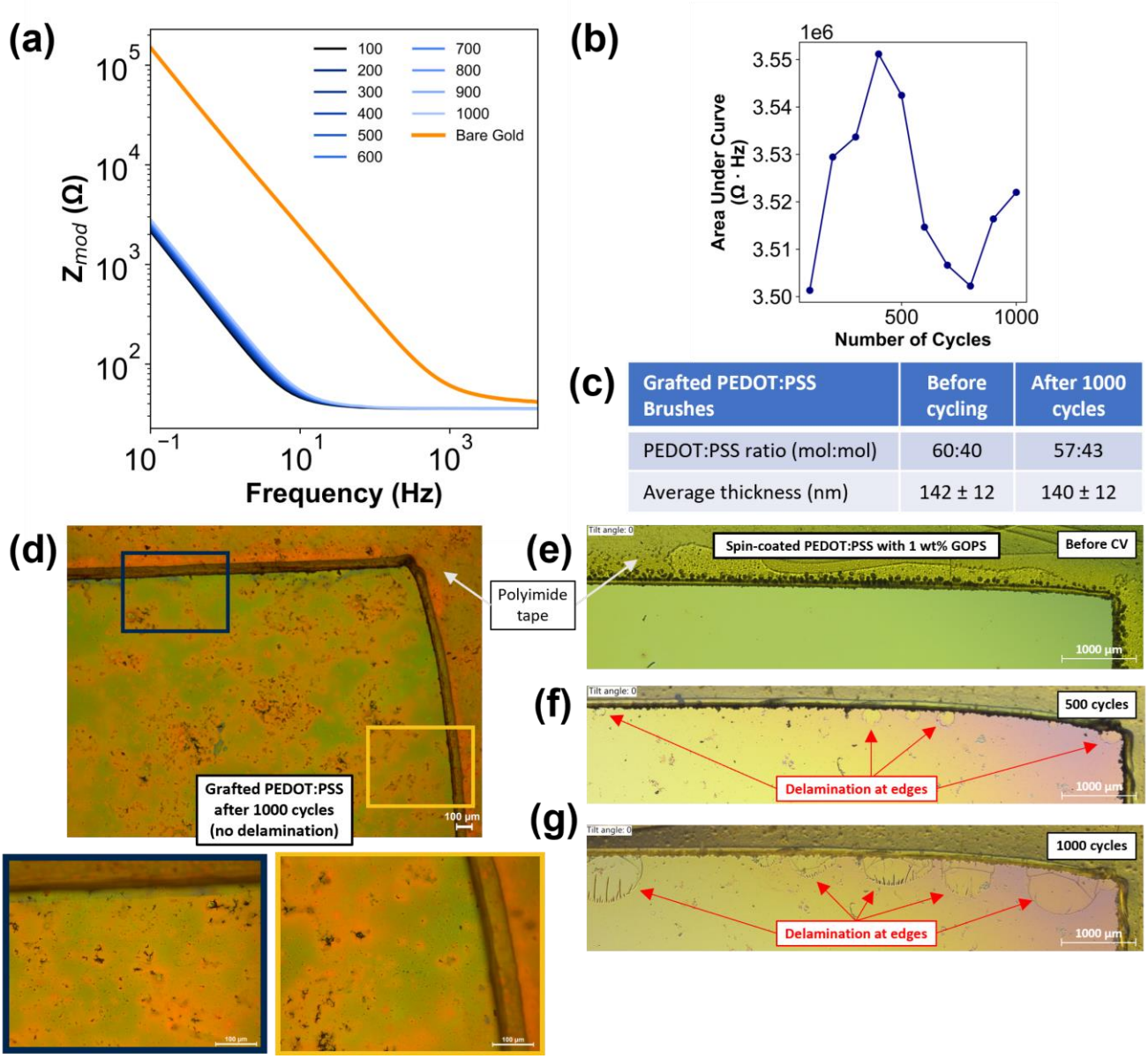

Figure 5. (a) EIS of grafted PEDOT:PSS compared to bare gold after 1000 cycles, sweeping from -0.4 to 0.8 V in PBS. At all frequencies ranging from 0.1 to 10^5 Hz, PEDOT:PSS surfaces have a significantly lower impedance, even after 1000 cycles. The stability of the integrated area under the curve for the first 1000 cycles is highlighted in (b) and demonstrates the stability of the PEDOT:PSS brushes to electrochemical cycling. (c) Integration of the S 2p XPS spectra before and after cycling 1000 scans in PBS shows almost no change in the ratio of PEDOT:PSS, while surface profilometry before and after cycling shows that film thickness is not significantly affected either. (d) Optical microscopy images of the grafted PEDOT:PSS brushes at various magnifications showed no cracks or signs of delamination after 1000 CV scans and demonstrate increased stability to electrochemical cycling compared to spin-coated and crosslinked Clevios™ PH1000 with 1 wt% GOPS, shown (e) before electrochemical cycling, (f) after 500 CV scans, and (g) after 1000 CV scans. Delamination in the spin-coated Clevios™ PH1000 sample can be seen from the appearance of round, bubble-like structures at the edge of the active area of the electrode.

minutes did not produce significant changes as evidenced by Raman spectroscopy or optical microscopy (**Supporting Information, Figure S2a-c**). As already mentioned, the stability of the grafted brushes was comparable to spin-coated and crosslinked Clevios™ PH1000 with 0.2 wt% GOPS, which also withstood 20 minutes of sonication (**Figure S2d-f**). (Clevios™ PH1000 without any additives, on the other hand, washes off of gold after lightly rinsing with water.)

Next, the stability of the PEDOT:PSS surfaces was evaluated with cyclic voltammetry (**Supporting Information, Figure S4**) and electrical impedance spectroscopy. The brushes were evaluated under physiologically relevant conditions (PBS) between 0.1 Hz to 10^5 Hz. The intended application of the PEDOT:PSS brushes is neural electrodes, so physiologically relevant conditions and frequencies (0.1–10 kHz) are of most interest. PEDOT:PSS significantly lowered the impedance of the gold surfaces at all frequencies ranging from 0.1 to 10^5 Hz even after 1000 cycles sweeping from -0.4 to 0.8 V, as shown in **Figure 5a**. The electrode appeared stable with minimal changes to the impedance up to 1000 cycles as shown in **Figure 5b** by the stability of the integrated area under the EIS

curves in **Figure 5a**. Integration of the S 2p XPS spectra before and after cycling 1000 scans in PBS (**Supporting Information, Figure S3**) shows almost no change in the ratio of PEDOT:PSS, and surface profilometry measurements do not appear to show any significant change in film thickness before and after cycling (**Figure 5c**). Optical microscopy of the grafted PEDOT:PSS brushes (**Figure 5d**) showed no cracks or signs of delamination even after 1000 cycles, compared to a spin-coated and crosslinked PEDOT:PSS sample (Clevios™ PH1000 with 1 wt% GOPS) that showed signs of delamination after only 500 cycles (**Figure 5f**) and significant delamination after 1000 cycles (**Figure 5g**). (Delamination was noted here by the appearance of round, bubble-like structures at the edge of the electrode active area.) While in theory the gold-thiol bond is susceptible to dissociation at higher temperatures and the ester linkage is susceptible to hydrolysis over time, the stability of the grafted films to sonication and cyclic electrical loading suggests that the films should remain intact for even longer durations under (less harsh) physiological conditions.

While it is difficult to accurately compare the impedance values in this work to impedances reported for microelectrode arrays due to the non-linear scaling of impedance with area and the dominance of edge effects for small microelectrode dimensions[51,52], film conductivities can be much more easily compared to literature values. Using the four-point probe method, the 100% and 90% grafting density samples had average conductivities of 2.8 and 2.6 S cm^{-1}, respectively. In comparison, spin-coated Clevios™ PH1000 with 0.2 wt% GOPS on gold had an average conductivity of 1.3 S cm^{-1} (**Supporting Information, Figure S5**). These results demonstrate the robustness of this approach to obtain conductive PEDOT films on noble metal surfaces that are stable to various stress conditions.

We demonstrated PSS grafted from a gold surface via surface-initiated ATRP could be used as a scaffold for PEDOT to produce PEDOT:PSS brushes with decreased impedance relative to bare gold and increased stability and conductivity compared to spin-coated analogs. Specifically, the PEDOT:PSS brushes were stable under sonication and withstood up to 1000 cycles of cyclic voltammetry without delaminating, compared to spin-coated PEDOT:PSS which delaminated completely during sonication and partially after 500 cycles of cyclic voltammetry. EIS measurements after every 100 cycles showed the samples had low impedances even lower than bare gold at all frequencies ranging from 0.1 to 10^5 Hz. We believe that the increased stability, increased conductivity, and lowered impedance makes SI-ATRP PEDOT:PSS a promising candidate for use in microelectrodes for neural activity recording. Spin-coated, electrodeposited, and drop-cast PEDOT:PSS have already been shown to reduce impedance and improve biocompatibility of microelectrodes. Instead of modifying the metal electrode or introducing crosslinkers or other additives to the polymer film, this work takes an organic chemistry and polymer approach to improving the stability of PEDOT:PSS layers on gold surfaces by chemically binding the polymer to the surface.

ASSOCIATED CONTENT

Supporting Information

The Supporting Information is available free of charge on the ACS Publications website.

Experimental section, Raman spectra, optical microscope images, XPS spectra, cyclic voltammograms (PDF)

AUTHOR INFORMATION

Corresponding Author

Darren J. Lipomi — Department of NanoEngineering, University of California, San Diego, 9500 Gilman Dr, Mail Code *0448, La Jolla, CA 92093-0448, USA*; Email: dlipomi@ucsd.edu

Author Contributions

The manuscript was written through contributions of all authors.

Notes

The authors declare no competing financial interests.

ACKNOWLEDGMENT

This work was supported by a grant from the National Science Foundation, award number CBET-2223566 to D. J. L. Additional support was provided by member companies of the Center for Wearable Sensors at UC San Diego: Dexcom, Google, Gore, Honda, Kureha, Merck KGaA, PepsiCo, Roche, Samsung, Sony, and Werfen. R. B. acknowledges that this project has received funding from the European Union's Horizon 2020 research and innovation programme under the Marie Skłodowska-Curie grant agreement No 898571. S. A. D. acknowledges support from the National Institutes of Health BRAIN initiative, grant numbers R01NS123655-01 and UG3NS123723-01. XPS characterization was carried out on an instrument acquired with funds from the U.S. National Science Foundation under their Major Research Instrumentation Program, grant number DMR-0958796.

REFERENCES

(1) Kipke, D. R.; Shain, W.; Buzsáki, G.; Fetz, E.; Henderson, J. M.; Hetke, J. F.; Schalk, G. Advanced Neurotechnologies for Chronic Neural Interfaces: New Horizons and Clinical Opportunities. *J. Neurosci.* **2008**, *28* (46), 11830–11838. https://doi.org/10.1523/jneurosci.3879-08.2008.

(2) Hatsopoulos, N. G.; Donoghue, J. P. The Science of Neural Interface Systems. *Annu. Rev. Neurosci.* **2009**, *32*, 249–266. https://doi.org/10.1146/annurev.neuro.051508.135241.

(3) Kozai, T. D. Y.; Langhals, N. B.; Patel, P. R.; Deng, X.; Zhang, H.; Smith, K. L.; Lahann, J.; Kotov, N. A.; Kipke, D. R. Ultrasmall Implantable Composite Microelectrodes with Bioactive Surfaces for Chronic Neural Interfaces. *Nat. Mater.* **2012**, *11* (12), 1065–1073. https://doi.org/10.1038/nmat3468.

(4) Cogan, S. F. Neural Stimulation and Recording Electrodes. *Annu. Rev. Biomed. Eng.* **2008**, *10*, 275–309. https://doi.org/10.1146/annurev.bioeng.10.061807.160518.

(5) Chen, R.; Canales, A.; Anikeeva, P. Neural Recording and Modulation Technologies. *Nat. Rev. Mat.* **2017**, *2*, 16093. https://doi.org/10.1038/natrevmats.2016.93.

(6) Ganji, M.; Tanaka, A.; Gilja, V.; Halgren, E.; Dayeh, S. A. Scaling Effects on the Electrochemical Stimulation Performance of Au, Pt, and PEDOT:PSS Electrocorticography Arrays. *Adv. Funct. Mater.* **2017**, *27* (42), 1703019. https://doi.org/10.1002/adfm.201703019.

(7) Ganji, M.; Kaestner, E.; Hermiz, J.; Rogers, N.; Tanaka, A.; Cleary, D.; Lee, S. H.; Snider, J.; Halgren, M.; Cosgrove, G. R.; Carter, B. S.; Barba, D.; Uguz, I.; Malliaras, G. G.; Cash, S. S.; Gilja, V.; Halgren, E.; Dayeh, S. A. Development and Translation of PEDOT:PSS Microelectrodes for Intraoperative Monitoring. *Adv. Funct. Mater.* **2018**, *28* (12), 1700232. https://doi.org/10.1002/adfm.201700232.

(8) Aqrawe, Z.; Montgomery, J.; Travas-Sejdic, J.; Svirskis, D. Conducting Polymers for Neuronal Microelectrode Array Recording and Stimulation. *Sens. Actuators B Chem.* **2018**, *257*, 753–765. https://doi.org/10.1016/j.snb.2017.11.023.

(9) Zhang, Z.; Tian, G.; Duan, X.; Chen, H.; Kim Richie, D.-H. Nanostructured PEDOT Coatings for Electrode–Neuron Integration. *ACS Appl. Bio Mater.* **2021**, *4* (7), 5556–5565. https://doi.org/10.1021/acsabm.1c00375.

(10) Nick, C.; Thielemann, C.; Schlaak, H. F. PEDOT:PSS Coated Gold Nanopillar Microelectrodes for Neural Interfaces. In *2014 International Conference on Manipulation, Manufacturing and Measurement on the Nanoscale (3M-NANO)*; 2014; pp 160–165. https://doi.org/10.1109/3M-NANO.2014.7057309.

(11) Pranti, A. S.; Schander, A.; Bödecker, A.; Lang, W. PEDOT: PSS Coating on Gold Microelectrodes with Excellent Stability and High Charge Injection Capacity for Chronic Neural Interfaces. *Sens. Actuators B Chem.* **2018**, *275*, 382–393. https://doi.org/10.1016/j.snb.2018.08.007.

(12) Venkatraman, S.; Hendricks, J.; King, Z. A.; Sereno, A. J.; Richardson-Burns, S.; Martin, D.; Carmena, J. M. In Vitro and In Vivo Evaluation of PEDOT Microelectrodes for Neural Stimulation and Recording. *IEEE Trans. Neural Syst. Rehabil. Eng.* **2011**, *19* (3), 307–316. https://doi.org/10.1109/TNSRE.2011.2109399.

(13) Abidian, M. R.; Martin, D. C. Experimental and Theoretical Characterization of Implantable Neural Microelectrodes Modified with Conducting Polymer Nanotubes. *Biomaterials* **2008**, *29* (9), 1273–1283. https://doi.org/10.1016/j.biomaterials.2007.11.022.

(14) Ganji, M.; Hossain, L.; Tanaka, A.; Thunemann, M.; Halgren, E.; Gilja, V.; Devor, A.; Dayeh, S. A. Monolithic and Scalable Au Nanorod Substrates Improve PEDOT–Metal Adhesion and Stability in Neural Electrodes. *Adv. Healthc. Mater.* **2018**, *7* (22), 1800923. https://doi.org/10.1002/adhm.201800923.

(15) Stavrinidou, E., Leleux, P., Rajaona, H., Khodagholy, D., Rivnay, J., Lindau, M., Sanaur, S. and Malliaras, G.G. (2013), Direct Measurement of Ion Mobility in a Conducting Polymer. Adv. Mater., 25: 4488-4493. https://doi.org/10.1002/adma.201301240.

(16) Berezhetska, O.; Liberelle, B.; Crescenzo, G. D.; Cicoira, F. A Simple Approach for Protein Covalent Grafting on Conducting Polymer Films. *J. Mater. Chem. B* **2015**, *3*, 5087–5094. https://doi.org/10.1039/c5tb00373c.

(17) Kergoat, L.; Piro, B.; Simon, D. T.; Pham, M. C.; Noël, V.; Berggren, M. Detection of Glutamate and Acetylcholine with Organic Electrochemical Transistors Based on Conducting Polymer/Platinum Nanoparticle Composites. *Adv. Mater.* **2014**, *26*, 5658–5664. https://doi.org/10.1002/adma.201401608

(18) Dijk, G.; Ruigrok, H. J.; O'Connor, R. P. Influence of PEDOT:PSS Coating Thickness on the Performance of Stimulation Electrodes. *Adv. Mater. Interfaces* **2020**, *7* (16), 200675. https://doi.org/10.1002/admi.202000675.

(19) Inoue, A.; Yuk, H.; Lu, B.; Zhao, X. Strong Adhesion of Wet Conducting Polymers on Diverse Substrates. *Sci. Adv.* **2020**, *6* (12), eaay5394. https://doi.org/10.1126/sciadv.aay5394.

(20) Solazzo, M.; Krukiewicz, K; Zhussupbekova, A.; Fleischer, K.; Biggs, M. J.; Monaghan, M. G. PEDOT:PSS Interfaces Stabilised Using a PEGylated Crosslinker Yield Improved Conductivity and Biocompatibility. *J. Mater. Chem. B* **2019**, *7* (31), 4811. https://doi.org/10.1039/C9TB01028A.

(21) Boehler, C.; Obereuber, F.; Schlabach, S.; Stieglitz, T.; Asplund, M. Long-Term Stable Adhesion for Conducting Polymers in Biomedical Applications: IrOx and Nanostructured Platinum Solve the Chronic Challenge. *ACS Appl. Mater. Interfaces* **2017**, *9*, 189–197. https://doi.org/10.1021/acsami.6b13468.

(22) Ouyang, L.; Wei, B.; Kuo, C.; Pathak, S.; Farrell, B.; Martin, D. C. Enhanced PEDOT Adhesion on Solid Substrates with Electrografted P(EDOT-NH_2). *Sci Adv.* **2017**, *3*, e1600448. https://doi.org/10.1126/sciadv.1600448.

(23) Belanger, D.; Pinson, J. Electrografting: A Powerful Method for Surface Modification. *Chem. Soc. Rev.* **2011**, *40,* 3995–4048. https://doi.org/10.1039/C0CS00149J.

(24) Zorn, G.; Baio, J. E.; Weidner, T.; Migonney, V.; Castner, D. G. Characterization of Poly(Sodium Styrene Sulfonate) Thin Films Grafted from Functionalized Titanium Surfaces. *Langmuir ACS J. Surf. Colloids* **2011**, *27* (21), 13104–13112. https://doi.org/10.1021/la201918y.

(25) Tran, Y.; Auroy, P. Synthesis of Poly(Styrene Sulfonate) Brushes. *J. Am. Chem. Soc.* **2001**, *123* (16), 3644–3654. https://doi.org/10.1021/ja992562s.

(26) Foster, R. N.; Johansson, P. K.; Tom, N. R.; Koelsch, P.; Castner, D. G. Experimental Design and Analysis of Activators Regenerated by Electron Transfer-Atom Transfer Radical Polymerization Experimental Conditions for Grafting Sodium Styrene Sulfonate from Titanium Substrates. *J. Vac. Sci. Technol. A* **2015**, *33* (5), 05E131. https://doi.org/10.1116/1.4929506.

(27) Foster, R. N.; Harrison, E. T.; Castner, D. G. ToF-SIMS and XPS Characterization of Protein Films Adsorbed onto Bare and Sodium Styrenesulfonate-Grafted Gold Substrates. *Langmuir* **2016**, *32* (13), 3207–3216. https://doi.org/10.1021/acs.langmuir.5b04743.

(28) Mulfort, K. L.; Ryu, J.; Zhou, Q. Preparation of Surface Initiated Polystyrenesulfonate Films and PEDOT Doped by the Films. *Polymer* **2003**, *44* (11), 3185–3192. https://doi.org/10.1016/S0032-3861(03)00247-7.

(29) Yasumoro, K.; Fujita, Y.; Arimatsu, H.; Fujima, T. A New Composite Structure of PEDOT/PSS: Macro-Separated Layers by a Polyelectrolyte Brush. *Polymers* **2020**, *12* (2), 456. https://doi.org/10.3390/polym12020456.

(30) Wolski, K.; Smenda, J.; Grobelny, A.; Dabczynski, P.; Marzec, M.; Cernescu, A.; Wytrwal, M.; Bernasik, A.; Rysz, J.; Zapotoczny, S. Surface Engineering of Mixed Conjugated/Polyelectrolyte Brushes – Tailoring Interface Structure and Electrical Properties. *J. Colloid Interface Sci.* **2023**, *634*, 209–220. https://doi.org/10.1016/j.jcis.2022.11.155.

(31) Jones, D. M.; Brown, A. A.; Huck, W. T. S. Surface-Initiated Polymerizations in Aqueous Media: Effect of Initiator Density. *Langmuir* **2002**, *18* (4), 1265–1269. https://doi.org/10.1021/la011365f.

(32) Park, C. S.; Lee, H. J.; Jamison, A. C.; Lee, T. R. Robust Thick Polymer Brushes Grafted from Gold Surfaces Using Bidentate Thiol-Based Atom-Transfer Radical Polymerization Initiators. *ACS Appl. Mater. Interfaces* **2016**, *8* (8), 5586–5594. https://doi.org/10.1021/acsami.5b11305.

(33) Rakhmatullina, E.; Braun, T.; Kaufmann, T.; Spillmann, H.; Malinova, V.; Meier, W. Functionalization of Gold and Silicon Surfaces by Copolymer Brushes Using Surface-Initiated ATRP. *Macromol. Chem. Phys.* **2007**, *208* (12), 1283–1293. https://doi.org/10.1002/macp.200700119.

(34) Kim, J.-B.; Bruening, M. L.; Baker, G. L. Surface-Initiated Atom Transfer Radical Polymerization on Gold at Ambient Temperature. *J. Am. Chem. Soc.* **2000**, *122* (31), 7616–7617. https://doi.org/10.1021/ja001652q.

(35) Mohammadi Sejoubsari, R.; Martinez, A. P.; Kutes, Y.; Wang, Z.; Dobrynin, A. V.; Adamson, D. H. "Grafting-Through": Growing Polymer Brushes by Supplying Monomers through the Surface. *Macromolecules* **2016**, *49* (7), 2477–2483. https://doi.org/10.1021/acs.macromol.6b00183.

(36) Iddon, P. D.; Robinson, K. L.; Armes, S. P. Polymerization of Sodium 4-Styrenesulfonate via Atom Transfer Radical Polymerization in Protic Media. *Polymer* **2004**, *45* (3), 759–768. https://doi.org/10.1016/j.polymer.2003.11.030.

(37) Matyjaszewski, K.; Dong, H.; Jakubowski, W.; Pietrasik, J.; Kusumo, A. Grafting from Surfaces for "Everyone": ARGET ATRP in the Presence of Air. *Langmuir* **2007**, *23* (8), 4528–4531. https://doi.org/10.1021/la063402e.

(38) Simakova, A.; Averick, S. E.; Konkolewicz, D.; Matyjaszewski, K. Aqueous ARGET ATRP. *Macromolecules* **2012**, *45* (16), 6371–6379. https://doi.org/10.1021/ma301303b.

(39) Jakubowski, W.; Min, K.; Matyjaszewski, K. Activators Regenerated by Electron Transfer for Atom Transfer Radical Polymerization of Styrene. *Macromolecules* **2006**, *39* (1), 39–45. https://doi.org/10.1021/ma0522716.

(40) Yan, C.-N.; Xu, L.; Liu, Q.-D.; Zhang, W.; Jia, R.; Liu, C.-Z.; Wang, S.-S.; Wang, L.-P.; Li, G. Surface-Induced ARGET ATRP for Silicon Nanoparticles with Fluorescent Polymer Brushes. *Polymers* **2019**, *11* (7), 1228. https://doi.org/10.3390/polym11071228.

(41) Choi, C.-K.; Kim, Y.-B. Atom Transfer Radical Polymerization of Styrenesulfonic Acid Sodium Salts (SSNa) in Aqueous Phase. *Polym. Bull.* **2003**, *49* (6), 433–439. https://doi.org/10.1007/s00289-003-0130-7.

(42) Sankhe, A. Y.; Husson, S. M.; Kilbey, S. M. Direct Polymerization of Surface-Tethered Polyelectrolyte Layers in Aqueous Solution via Surface-Confined Atom Transfer Radical Polymerization. *J. Polym. Sci. Part Polym. Chem.* **2007**, *45* (4), 566–575. https://doi.org/10.1002/pola.21817.

(43) Foster, R. N.; Keefe, A. J.; Jiang, S.; Castner, D. G. Surface Initiated Atom Transfer Radical Polymerization Grafting of Sodium Styrene Sulfonate from Titanium and Silicon Substrates. *J. Vac. Sci. Technol. A* **2013**, *31* (6), 06F103. https://doi.org/10.1116/1.4819833.

(44) Bourg, M.-C.; Badia, A.; Lennox, R. B. Gold−Sulfur Bonding in 2D and 3D Self-Assembled Monolayers: XPS Characterization. *J. Phys. Chem. B* **2000**, *104* (28), 6562–6567. https://doi.org/10.1021/jp9935337.

(45) Yang, J. C.; Jablonsky, M. J.; Mays, J. W. NMR and FT-IR Studies of Sulfonated Styrene-Based Homopolymers and Copolymers. *Polymer* **2002**, *43* (19), 5125–5132. https://doi.org/10.1016/S0032-3861(02)00390-7.

(46) Falentin-Daudré, C.; Aitouakli, M.; Baumann, J. S.; Bouchemal, N.; Humblot, V.; Migonney, V.; Spadavecchia, J. Thiol-Poly(Sodium Styrene Sulfonate) (PolyNaSS-SH) Gold Complexes: From a Chemical Design to a One-Step Synthesis of Hybrid Gold Nanoparticles and Their Interaction with Human Proteins. *ACS Omega* **2020**, *5* (14), 8137–8145. https://doi.org/10.1021/acsomega.0c00376.

(47) Hwang, J.; Amy, F.; Kahn, A. Spectroscopic Study on Sputtered PEDOT·PSS: Role of Surface PSS Layer. *Org. Electron.* **2006**, *7* (5), 387–396. https://doi.org/10.1016/j.orgel.2006.04.005.

(48) Crispin, X.; Marciniak, S.; Osikowicz, W.; Zotti, G.; van der Gon, A. W. D.; Louwet, F.; Fahlman, M.; Groenendaal, L.; De Schryver, F.; Salaneck, W. R. Conductivity, Morphology, Interfacial Chemistry, and Stability of Poly(3,4-Ethylene Dioxythiophene)–Poly(Styrene Sulfonate): A Photoelectron Spectroscopy Study. *J. Polym. Sci. Part B Polym. Phys.* **2003**, *41* (21), 2561–2583. https://doi.org/10.1002/polb.10659.

(49) Zotti, G.; Zecchin, S.; Schiavon, G.; Louwet, F.; Groenendaal, L.; Crispin, X.; Osikowicz, W.; Salaneck, W.; Fahlman, M. Electrochemical and XPS Studies toward the Role of Monomeric and Polymeric Sulfonate Counterions in the Synthesis, Composition, and Properties of Poly(3,4-Ethylenedioxythiophene). *Macromolecules* **2003**, *36* (9), 3337–3344. https://doi.org/10.1021/ma021715k.

(50) Shahrim, N. A.; Ahmad, Z.; Azman, A. W.; Buys, Y. F.; Sarifuddin, N. Mechanisms for Doped PEDOT:PSS Electrical Conductivity Improvement. *Mater. Adv.* **2021**, *2*, 7118–7138. https://doi.org/10.1039/d1ma00290b.

(51) Vatsyayan, R.; Dayeh, S. A. A Universal Model of Electrochemical Safety Limits In Vivo for Electrophysiological Stimulation. *Front. Neurosci.* **2022**, *16*, 972252. https://doi.org/10.3389/fnins.2022.972252.

(52) Ganji, M.; Elthakeb, A. T.; Tanaka, A.; Gilja, V.; Halgren, E.; Dayeh, S. A. Scaling Effects on the Electrochemical Performance of Poly(3,4-Ethylenedioxythiophene (PEDOT), Au, and Pt for Electrocorticography Recording. *Adv. Funct. Mater.* **2017**, *27*, 1703018. https://doi.org/10.1002/adfm.201703018.

For Table of Contents use only:

Synthesis of PEDOT:PSS Brushes Grafted from Gold Using ATRP for Increased Electrochemical and Mechanical Stability

Jason X. Tuermer-Lee, Allison Lim, Louis Ah, Rachel Blau, Yi Qie, Wade Shipley, Laure V. Kayser, Samantha M. Russman, Andrea R. Tao, Shadi A. Dayeh, and Darren J. Lipomi*